



Improved energy transfer process in BaZrO₃:Eu³⁺ nanophosphor synthesized by Sol-gel technique

Subhash Chand*, S.P. Khatkar and Ishwar Singh

Department of Chemistry, M.D. University, Rohtak-124001, Haryana, India
drs Chopra78@gmail.com

Available online at: www.isca.in, www.isca.me

Received 3rd March 2018, revised 2nd July 2018, accepted 14th July 2018

Abstract

The BaZrO₃ doped with europium(III) and codoped with alkali ions (Li⁺, Na⁺ and K⁺) nanophosphor series was prepared by sol-gel synthesis. The materials thus obtained were heated to 1050^oC to improve the crystallinity and their morphology was examined by X-ray diffraction and scanning electron microscopy respectively. XRD spectra showed perovskite cubic structure for the materials BaZrO₃:Eu³⁺, M⁺ (M=Li⁺, Na⁺, K⁺) having smooth and regular surface. The phosphors emitted red color and the emission were due to ⁵D₀→⁷F_J transitions of Eu³⁺ ions where J = 0, 1, 2, 3, 4, respectively. BaZrO₃:Eu³⁺ possessed strong transition at ⁵D₀→⁷F_J (J = 1, 2) with peak located at 595 and 612 nm respectively. The improved photoluminescence intensity corresponding to ⁵D₀→⁷F₁ and ⁵D₀→⁷F₂ was observed if the BaZrO₃:Eu³⁺ phosphor is codoped with Li⁺ ions in addition to a broad band composed of many peaks between 440 to 575 nm was also observed.

Keywords: BaZrO₃:Eu³⁺; M (M=Li⁺, Na⁺, K⁺); Perovskites, Sol gel synthesis; Photoluminescence.

Introduction

Rare earth ion doped perovskite-type phosphors¹⁻⁶ have outstanding light emitting property⁷⁻¹². Barium zirconate phosphors have interesting light emitting properties with excellent thermo-mechanical properties and also fluid application in aerospace technologies¹³. BaZrO₃ itself has a protective action against corrosion in superconductors¹⁴⁻¹⁶. This perovskite material is a highly refractory melting between 2600 to 2700^oC and fluid application in fuel cells and proton conductors^{17,18}. Its band gap depend on the synthesis method and varies between 3.8 and 5 eV¹⁹ and therefore is the best crucible materials for crystal growth²⁰⁻²¹. The material shows low thermal conductivity, high dielectric constant and highly stable mechanically as well as structurally at high temperatures^{22,23}. With these outstanding properties, BaZrO₃ find itself as a capable contender for thermal coatings in aerospace application²². When doped with optical centre such as Eu(III), BaZrO₃ became a potential phosphor material because of its high thermal stability and wide band gap²³⁻²⁶. However BaZrO₃ doped with rare earths had been synthesized by different methods^{13,27-32}, we had applied the sol gel method to prepare BaZrO₃:Eu³⁺ phosphors. Further addition of alkali metal ion increased the photoluminescence possibly, as a charge compensator³³ of europium ion in the BaZrO₃ host lattice and therefore doping of Eu(III) ion with codoping of alkali metal ion have been proposed to be a highly BaZrO₃ lattice.

Materials and methods

Synthesis of nano-phosphors: High purity (99.9%) chemicals like Ba(NO₃)₂, Zr(NO₃)₄ [1mol], Eu(NO₃)₃, NaNO₃, KNO₃, LiNO₃, and citric acid (C₆H₈O₇) from Aldrich were used to

prepare a series of nano-materials having general formula Ba_(1-x)ZrO₃:xEu³⁺ and Ba_(1-x+y)ZrO₃:xEu³⁺, yM (M=Li⁺, Na⁺, K⁺) where x is 5mol% and y is 1mol% were prepared by heating slowly an aqueous concentrated mixture containing a calculated amount of metal nitrates and citric acid on a magnetic stirrer maintained at 150^oC. The mixture undergoes slow dehydration and resulting viscous gel calcined inside muffle furnace maintained at 1050^oC for 3h to increase the crystallinity of the product.

Characterization of phosphor: Photoluminescence properties (PL) were determined in back scattering geometry with a 325nm He-Cd laser and the emission spectra were obtained by a HR-4000 Ocean Optics USB spectrometer. For analyzing the PL properties the synthesized material were pressed into pellets with a size 10 mm diameter /1 mm thickness. The morphology of the phosphors were investigated by scanning electron microscopy (SEM) using a JEOL JSM6300 SEM microscope operating at 10 kV. The crystal structure characterization was performed by high resolution X-ray diffraction (XRD) using Rigaku Ultima IV diffractometer in the θ -2 θ configuration and using Cu K α radiation (0.154184nm). All measurements were carried out at room temperature.

Results and discussion

Crystal structure determination: Figure-1(a) contain XRD spectra of BaZrO₃:Eu³⁺, M (M = Li⁺, Na⁺ and K⁺) phosphors synthesized by sol-gel technique and confirming the presence of extra phase like ZrO₂[JCPDS No. 37-1484], Eu₂Zr₂O₇[JCPDS No. 24-0418], and Eu₂O₃[JCPDS No. 34-0072] along with main product BaZrO₃[JCPDS 06-0399]. Main XRD peaks of Eu³⁺ doped BaZrO₃ strongly confirm the accommodation of Ba²⁺

sites by the Eu^{3+} ions thus confirming its increased height and photoluminescence property. When Ba^{2+} ions are replaced by Eu^{3+} ions, the lattice structure do not change so much as evidenced from the XRD spectra of $\text{BaZrO}_3:\text{Eu}^{3+}$ but slight variation were observed due to little difference in the ionic radii of Eu^{3+} (0.0947 nm) and that of Ba^{2+} (0.135 nm)³⁴.

The entire diffraction peaks match with the JCPDS card no. 06-0399, space group $Pm\bar{3}m$ (221) data. BaZrO_3 possessed cubic structure as shown in Figure-1(b) having unit cell geometry with axis i.e. $a = b = c = 0.4193\text{nm}$ and axial angles $\alpha = \beta = \gamma = 90^\circ$. The prepared nano-materials have general formula $\text{Ba}_{(1-x)}\text{ZrO}_3:\text{Eu}^{3+}$ where Ba^{2+} ions were substituted by Eu^{3+} ions during their doping in host matrix. But the probability of substitution of Eu^{3+} ions by Zr^{4+} ions is not possible due to large ionic size difference between Zr^{4+} (0.072nm, coordination number = 6) and that of Eu^{3+} (0.0947nm) ions as supported by Lui et al.³⁵.

Increased^{36,37} in the cell volume of the host matrix was observed if larger anions substituted by the smaller cations in the crystalline lattice. Corresponding unit cell constants and unit cell volumes of $\text{BaZrO}_3:\text{Eu}^{3+}$ and $\text{BaZrO}_3:\text{Eu}^{3+}$ co-doped with Li^+ , Na^+ , K^+ ions calculated from the distance between the adjacent (110) planes corresponding to direction peaks near $2\theta = 30.13^\circ$ are listed in Table-1. The substitution of Li^+ at Zr^{4+} site would be possible if only size was under consideration but here charge difference between Li^+ and Zr^{4+} is quite large and its substitution causes more point defects in crystallites, resulting decreased in PL properties of $\text{BaZrO}_3:\text{Eu}^{3+}$ materials. Hence the PL intensity increased considerably with the co-doping with Li^+ ions in the $\text{BaZrO}_3:\text{Eu}^{3+}$, where the substitution of Li^+ at Ba^{2+} sites or at interstitial positions very suitable for consideration.

Surface morphology and particle size examination: Crystal structure, particle size and surface roughness of the phosphor have significant effects on the photoluminescence intensity.

Table-1: Calculated lattice parameters of $\text{BaZrO}_3:\text{Eu}^{3+}$ co-doped with Li^+ , Na^+ and K^+ .

Phosphors	a/nm	b/nm	c/nm	v/nm	Crystallite size/nm
$\text{BaZrO}_3:\text{Eu}^{3+}$	0.4193	0.4193	0.4193	0.0737	20nm
$\text{BaZrO}_3:\text{Eu}^{3+},\text{Li}^+$	0.4189	0.4189	0.4189	0.0735	10nm
$\text{BaZrO}_3:\text{Eu}^{3+},\text{Na}^+$	0.4193	0.4193	0.4193	0.0735	20nm
$\text{BaZrO}_3:\text{Eu}^{3+},\text{K}^+$	0.4197	0.4197	0.4197	0.0738	20nm

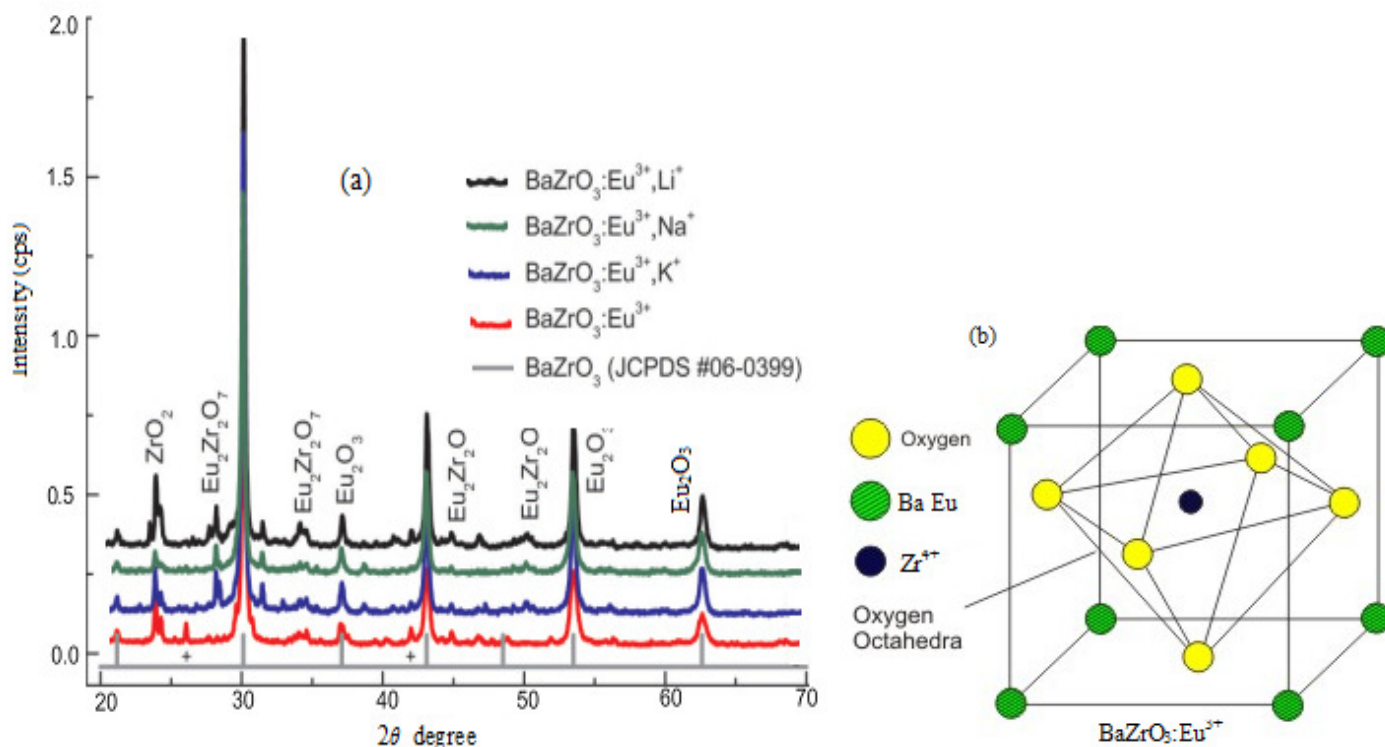


Figure-1: XRD patterns of (a) $\text{BaZrO}_3:\text{Eu}^{3+}$ co-doped with Li^+ , Na^+ and K^+ (b) Cubic structure of $\text{BaZrO}_3:\text{Eu}^{3+}$

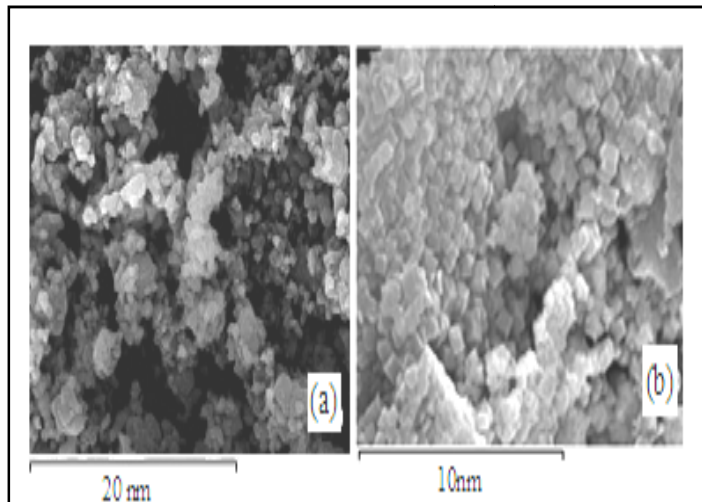


Figure-2: SEM images of doped particles (a) BaZrO₃:Eu³⁺ (b) BaZrO₃:Eu³⁺, Li⁺.

In Figure-2(b), the SEM micrograph of BaZrO₃ doped with Eu³⁺ and the same co-doped with Li⁺ ions show fair uniformity with dense microstructures. The packed particles with nearly cubical shape were observed. The average size of BaZrO₃ doped with Eu³⁺ and the same co-doped with Li⁺ ions crystallites calculated from the main XRD peaks corresponding to 30.13° and was found to be 10 to 20nm. This show good agreement with the size of particles in their SEM images.

Photoluminescence determination: Figure-2 depict the room temperature emission spectra of BaZrO₃:Eu³⁺ and BaZrO₃:Eu³⁺,M [M= Li⁺, Na⁺, K⁺], obtained on excitation by ultraviolet light at 325 nm. The obtained products emitted the red luminescence of varying intensities peaking at 578, 598, 612, 650-671 and 701nm corresponding to ⁵D₀→⁷F₀, ⁵D₀→⁷F₁, ⁵D₀→⁷F₂, ⁵D₀→⁷F₃, and ⁵D₀→⁷F₄ transitions³⁸ respectively, thus confirming that activator (Eu³⁺) had successfully entered the Ba²⁺ site of BaZrO₃ lattice.

The some particular bands for Eu³⁺ ions corresponding to many peaks between 440 and 575 nm has also been observed in the BaZrO₃:Eu³⁺. The intensity of this band is maximum in Li⁺ co-doped sample and minimum for K⁺ doped ions. The exact positions of emission peaks in various lattices are shown in Table-2. It was observed that luminescence peaks of Eu³⁺ are very sensitive to the symmetry around Eu³⁺ ions. Mostly the PL intensity ratio of I(⁵D₀→⁷F₂) to I(⁵D₀→⁷F₁) used to determine the environmental symmetry around Eu³⁺ ion the host matrix³⁷ and the calculated the intensity ratio i.e. I(⁵D₀→⁷F₂) / I(⁵D₀→⁷F₁) for BaZrO₃:Eu³⁺ co-doped with alkali metal ions was found nearly same as shown in Table-2, thus confirming better the symmetry around Eu³⁺ in BaZrO₃ lattice and also in strong evidenced with the XRD results obtained. The number of peaks in the same wavelength region had also been observed in CaZrO₃:Eu³⁺, Mg²⁺ and LaAlO₃:Eu³⁺, Li⁺ materials^{39,40}. These emission lines were assigned to the f-f transitions of ⁵D₃→⁷F₄,

⁵D₂→⁷F_J (J = 1, 2, 3), ⁵D₁→⁷F_J (J = 1, 2). The increased PL intensity follows the order: Li⁺ > Na⁺ > K⁺ when co-doped in BaZrO₃:Eu³⁺. As the role of charge compensators to decrease the intrinsic defects as well as to enhance the energy transfer from host to charge transfer states had already investigated⁴¹⁻⁴⁴. Mari *et al*⁴⁵ observed that the incorporating of mono-valent ions in CaTiO₃:Pr³⁺ creates oxygen vacancies, which might act as a sensitizer for effective energy transfer due to strong mixing of charge transfer states. Further, co-doping of the monovalent ions also improve the morphology and particle size of the phosphors. The increased in the crystallinity also increase the oscillating strength for optical transitions. It was observed that mono-valent ion co-doping not only decreases the surface defects but also enhanced the energy transfer process from host to Eu³⁺. In the present work, because of the small size of Li⁺ ion, Li⁺ ion proved itself the most effective compensator for Eu³⁺. As the sizes of Na⁺ and K⁺ are comparable to the size of Ba²⁺, so they will occupy the Ba sites. Due to quite small size, Li⁺ ion entry in the interstitial site is also equally possible thus further facilitate the energy transfer from host lattice to Eu³⁺ centers. The evidence of interstitial substitution has already been obtained from the decrease of cell volumes of Li⁺ doped BaZrO₃:Eu³⁺ lattices.

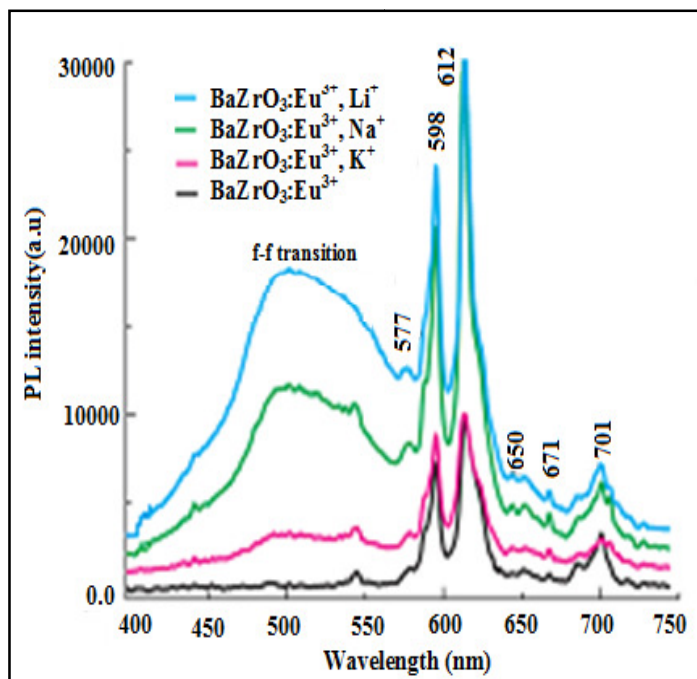


Figure-3: Photoluminescence spectra of BaZrO₃:Eu³⁺ co-doped with Li⁺, Na⁺, K⁺ ions.

Color purity determination: The color coordinates diagram of the BaZrO₃:Eu³⁺ obtained by spectroscopic method had been shown in Figure-4. The color co-ordinates for (5mol% Eu³⁺) BaZrO₃:Eu³⁺,Li⁺ are x = 0.665 and y = 0.330. These coordinates are very near to the red light emission. Hence this phosphor having excellent color purity and tenability from red light emission.

Table-2: Exact position of emission peaks (nm).

Phosphors	$^5D_0 \rightarrow ^7F_0$	$^5D_0 \rightarrow ^7F_1$	$^5D_0 \rightarrow ^7F_2$	$^5D_0 \rightarrow ^7F_3$	$^5D_0 \rightarrow ^7F_4$	$I_{(5D_0 \rightarrow 7F_2)} / I_{(5D_0 \rightarrow 7F_1)}$
BaZrO ₃ :Eu ³⁺	577-578	598	612	650-671	701	1.32
BaZrO ₃ :Eu ³⁺ ,Li ⁺	577-578	598	612	650-671	701	1.45
BaZrO ₃ :Eu ³⁺ ,Na ⁺	577-579	598	612	650-671	701	1.08
BaZrO ₃ :Eu ³⁺ , K ⁺	577-578	598	612	650-671	701	1.05

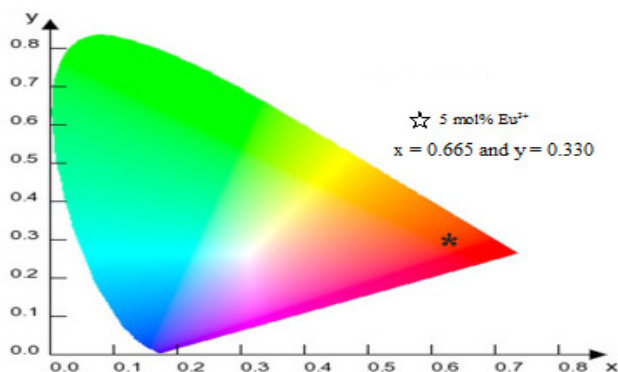


Figure-4: CIE chromaticity diagram of BaZrO₃:0.05Eu³⁺, 0.01Li⁺.

Conclusion

XRD examination of BaZrO₃:Eu³⁺, M (M= Li⁺, Na⁺, K⁺) nanophosphor prepared by sol-gel technique confirm the existence of cubic phase as main phase in BaZrO₃:Eu³⁺ materials. The average particle size of synthesized materials lies between 10 to 20nm. The increased in the red luminescence intensity by incorporation of monovalent charge compensators (Li⁺, Na⁺, K⁺) in BaZrO₃:Eu³⁺ phosphors is due to the decrease of radiationless energy transfer centers like the point defects and also due to easy energy transfer from host to Eu³⁺ ions. A remarkable increase in the photoluminescence intensity by codoping with Li⁺ metal ions in BaZrO₃:Eu³⁺ lattices make them promising as red luminescent nanomaterials for display applications.

Acknowledgments

Authors are highly thankful to Department of Chemistry, M.D. University, Rohtak-124001, Haryana, India for providing the chemical assistance and lab equipment essentially required for synthesis of this nanophosphor.

References

- Singh D., Tanwar V., Simantilleke A.P., Mari B., Kadyan P.S. and Singh I. (2016). Rapid synthesis and enhancement in down conversion emission properties of BaAl₂O₄: Eu²⁺, RE³⁺ (RE³⁺= Y, Pr) nanophosphors. *Journal of Materials Science: Materials in Electronics*, 27(3), 2260-2266.
- Singh D. and Singh I. (2016), *Advanced Magnetic and Optical Materials*, ed. by Tiwari A., Lyer P.K., Kumar V., Swart H., *Scrivener Publishing LLC*, Wiley.
- Huang J., Zhou L., Lan Y., Gong F., Li Q. and Sun J. (2011). Synthesis and luminescence properties of the red phosphor CaZrO₃: Eu³⁺ for white light-emitting diode application. *Central European Journal of Physics*, 9(4), 975-979.
- Boutinaud P., Pinel E., Dubois M., Vink A.P. and Mahiou R. (2005). UV-to-red relaxation pathways in CaTiO₃: Pr³⁺. *Journal of luminescence*, 111(1-2), 69-80.
- Singh D. and Kadyan S. (2017). Synthesis and optical characterization of trivalent europium doped M₄Al₂O₉ (M= Y, Gd and La) nanomaterials for display applications. *Journal of Materials Science: Materials in Electronics*, 28(15), 11142-11150.
- Zhang H.X., Kam C.H., Zhou Y., Han X.Q., Buddhudu S., Xiang Q. and Chan Y.C. (2000). Green upconversion luminescence in Er³⁺: BaTiO₃ films. *Applied Physics Letters*, 77(5), 609-611.
- Amami J., Hreniak D., Guyot Y., Pazik R., Goutaudier C., Boulon G. and Strek W. (2006). Second harmonic generation and Yb³⁺ cooperative emission used as structural probes in size-driven cubic-tetragonal phase transition in BaTiO₃ sol-gel nanocrystals. *Journal of luminescence*, 119, 383-387.
- Mari B., Singh I., Kadyan P.S. and Singh D. (2014), *Adv. Sci. Lett.*, 20 (7-8), 1531.
- Pinel E., Boutinaud P. and Mahiou R. (2004). What makes the luminescence of Pr³⁺ different in CaTiO₃ and CaZrO₃?. *Journal of alloys and compounds*, 380(1-2), 225-229.
- Singh D., Sheoran S., Tanwar V. and Bhagwan S. (2017). Optical characteristics of Eu (III) doped MSiO₃ (M= Mg, Ca, Sr and Ba) nanomaterials for white light emitting applications. *Journal of Materials Science: Materials in Electronics*, 28(4), 3243-3253.
- Zhang H., Fu X., Niu S. and Xin Q. (2008). Synthesis and photoluminescence properties of Eu³⁺-doped AZrO₃ (A=

- Ca, Sr, Ba) perovskite. *Journal of alloys and compounds*, 459(1-2), 103-106.
12. Alarcon J., Van der Voort D. and Blasse G. (1992). Efficient Eu³⁺ luminescence in non-lanthanide host lattices. *Materials research bulletin*, 27(4), 467-472.
 13. Liu X. and Wang X. (2007). Preparation and luminescence properties of BaZrO₃: Eu phosphor powders. *Optical Materials*, 30(4), 626-629.
 14. Erb A., Walker E. and Flükiger R. (1995). BaZrO₃: the solution for the crucible corrosion problem during the single crystal growth of high-Tc superconductors REBa₂Cu₃O_{7- δ} ; RE= Y, Pr. *Physica C: Superconductivity*, 245(3-4), 245-251.
 15. Liang R., Bonn D.A. and Hardy W.N. (1998). Growth of high quality YBCO single crystals using BaZrO₃ crucibles. *Physica C: Superconductivity*, 304(1-2), 105-111.
 16. Goretta K.C., Park E.T., Koritala R.E., Cuber M.M., Pascual E.A., Chen N. and Roubort J.L. (1998). Thermomechanical response of polycrystalline BaZrO₃. *Physica C: Superconductivity*, 309(3-4), 245-250.
 17. Tao S. and Irvine J.T. (2007). Conductivity studies of dense yttrium-doped BaZrO₃ sintered at 1325 C. *Journal of Solid State Chemistry*, 180(12), 3493-3503.
 18. Yuan Y., Zhang X., Liu L., Jiang X., Lv J., Li Z. and Zou Z. (2008). Synthesis and photocatalytic characterization of a new photocatalyst BaZrO₃. *International journal of hydrogen energy*, 33(21), 5941-5946.
 19. Cavalcante L.S., Longo V.M., Zampieri M., Espinosa J.W.M., Pizani P.S., Sambrano J.R. and Paskocimas C.A. (2008). Experimental and theoretical correlation of very intense visible green photoluminescence in Ba Zr O 3 powders. *Journal of Applied Physics*, 103(6), 063527.
 20. D'Alessandro F., Pacchiarotta G., Rubino A., Sperandio M., Villa P., Carrera A.M. and Congiu A. (2010). Lean catalytic combustion for ultra-low emissions at high temperature in gas-turbine burners. *Energy & Fuels*, 25(1), 136-143.
 21. Kirby N.M., van Riessen A., Buckley C.E. and Wittorff V.W. (2005). Oxalate-precursor processing for high quality BaZrO₃. *Journal of materials science*, 40(1), 97-106.
 22. Cervera R.B., Oyama Y., Miyoshi S., Kobayashi K., Yagi T. and Yamaguchi S. (2008). Structural study and proton transport of bulk nanograined Y-doped BaZrO₃ oxide protonics materials. *Solid State Ionics*, 179(7-8), 236-242.
 23. Vassen R., Cao X., Tietz F., Basu D. and Stöver D. (2000). Zirconates as new materials for thermal barrier coatings. *Journal of the American Ceramic Society*, 83(8), 2023-2028.
 24. van Duin A.C., Merinov B.V., Han S.S., Dorso C.O. and Goddard Iii W.A. (2008). ReaxFF reactive force field for the Y-doped BaZrO₃ proton conductor with applications to diffusion rates for multigranular systems. *The Journal of Physical Chemistry A*, 112(45), 11414-11422.
 25. Bhide S.V. and Virkar A.V. (1999). Stability of AB 1/2' B "1/2 O 3-Type Mixed Perovskite Proton Conductors. *Journal of the Electrochemical Society*, 146(12), 4386-4392.
 26. Münch W., Kreuer K.D., Seifert G. and Maier J. (2000). Proton diffusion in perovskites: comparison between BaCeO₃, BaZrO₃, SrTiO₃, and CaTiO₃ using quantum molecular dynamics. *Solid State Ionics*, 136, 183-189.
 27. Grinberg I. and Rappe A.M. (2004). Silver solid solution piezoelectrics. *Applied physics letters*, 85(10), 1760-1762.
 28. Shi C., Yoshino M. and Morinaga M. (2005). First-principles study of protonic conduction in In-doped AZrO₃ (A= Ca, Sr, Ba). *Solid State Ionics*, 176(11-12), 1091-1096.
 29. Romero V.H., De la Rosa E., Salas P. and Velazquez-Salazar J.J. (2012). Strong blue and white photoluminescence emission of BaZrO₃ undoped and lanthanide doped phosphor for light emitting diodes application. *Journal of Solid State Chemistry*, 196, 243-248.
 30. Borja-Urby R., Diaz-Torres L.A., Salas P., Vega-Gonzalez M. and Angeles-Chavez C. (2010). Blue and red emission in wide band gap BaZrO₃: Yb³⁺, Tm³⁺. *Materials Science and Engineering: B*, 174(1-3), 169-173.
 31. Singh V., Rai V.K., Al-Shamery K., Haase M. and Kim S.H. (2013). NIR to visible frequency upconversion in Er³⁺ and Yb³⁺ co-doped BaZrO₃ phosphor. *Spectrochimica Acta Part A: Molecular and Biomolecular Spectroscopy*, 108, 141-145.
 32. Borja-Urby R., Diaz-Torres L.A., Salas P., Angeles-Chavez C. and Meza O. (2011). Strong broad green UV-excited photoluminescence in rare earth (RE= Ce, Eu, Dy, Er, Yb) doped barium zirconate. *Materials Science and Engineering: B*, 176(17), 1388-1392.
 33. Marí B., Singh K.C., Moya M., Singh I., Om H. and Chand S. (2012). Characterization and photoluminescence properties of some CaO, SrO and CaSrO₂ phosphors co-doped with Eu³⁺ and alkali metal ions. *Optical Materials*, 34(8), 1267-1271.
 34. Guan L., Jin L.T., Guo S.Q. and Liu Y.F., (2010), *J. Rare Earths*, 28, 292.
 35. Hannan A., Iwasa K., Kohgi M. and Suzuki T. (2000). Crystal-lattice anomaly of CeSb under high pressure induced by magnetic polaron formation. *Journal of the Physical Society of Japan*, 69(7), 2358-2359.
 36. Ahmed M.A., Ateia E. and El-Dek S.I. (2003). Rare earth doping effect on the structural and electrical properties of Mg-Ti ferrite. *Materials Letters*, 57(26-27), 4256-4266.

37. Zhang H., Fu X., Niu S., Sun G. and Xin Q. (2004). Low temperature synthesis of nanocrystalline YVO₄: Eu via polyacrylamide gel method. *Journal of Solid State Chemistry*, 177(8), 2649-2654.
38. Lu Z., Chen L., Tang Y. and Li Y. (2005). Preparation and luminescence properties of Eu³⁺-doped MSnO₃ (M= Ca, Sr and Ba) perovskite materials. *Journal of Alloys and Compounds*, 387(1-2), L1-L4.
39. Mao Z.Y., Wang D.J., Lu Q.F., Yu W.H. and Yuan Z.H. (2009), *Chem. Commun.*, 346.
40. Shimizu Y., Sakagami S., Goto K., Nakachi Y. and Ueda K. (2009). Tricolor luminescence in rare earth doped CaZrO₃ perovskite oxides. *Materials Science and Engineering: B.*, 161(1-3), 100-103.
41. Blasse G. and Grabmaier B.C. (1994). A general introduction to luminescent materials. In *Luminescent materials*, Springer, Berlin, Heidelberg, 1-9.
42. Ryu H., Singh B.K., Bartwal K.S., Brik M.G. and Kityk I.V. (2008). Novel efficient phosphors on the base of Mg and Zn co-doped SrTiO₃: Pr³⁺. *Acta Materialia*, 56(3), 358-363.
43. Diallo P.T., Jeanlouis K., Boutinaud P., Mahiou R. and Cousseins J.C. (2001). Improvement of the optical performances of Pr³⁺ in CaTiO₃. *Journal of alloys and compounds*, 323, 218-222.
44. Tang J., Yu X., Yang L., Zhou C. and Peng X. (2006). Preparation and Al³⁺ enhanced photoluminescence properties of CaTiO₃: Pr³⁺. *Materials Letters*, 60(3), 326-329.
45. Marí B., Singh K.C., Cembrero-Coca P., Singh I., Singh D. and Chand S. (2013). Red emitting MTiO₃ (M= Ca or Sr) phosphors doped with Eu³⁺ or Pr³⁺ with some cations as co-dopants. *Displays*, 34(4), 346-351.